Simulation of Electromagnetic Field of a Fast Moving Target Close to Antennas

Filip Kozak, Miloslav Capek, Vojtech Jenik, Premysl Hudec and Zbynek Skvor

Czech Technical University in Prague, Faculty of Electrical Engineering, Department of Electromagnetic Field, Technicka 2, 166 27, Prague , Czech republic, kozakfi1@fel.cvut.cz

***Abstract*—Experiments have shown that Doppler signatures of a missile moving in a close vicinity of the antenna is quite complex. Experimentally obtained spectrograms exhibit clusters of Doppler frequencies instead of a single one. This is due to the fact that radial velocities differ significantly for different parts of the missile. Partial numerical simulations of this complex problem have been carried out for thin long fast-moving targets (wires). Simulation results compare well with measured Doppler signatures and enable better understanding of the problem and therefore improve the ability to distinguish dangerous targets from ordinary ones.**

***Index Terms*—Doppler signatures, Doppler frequency shift, fast-moving target, near-zone, active defense, elementary dipole.**

I. Introduction

The Active Defense System (ADS) represents a modern solution for military vehicles protection against many types of threat missiles. ADS solve these problems by detecting the approaching missiles and activating suitable counter-measures. Besides being cheaper and lighter, they should provide substantially higher degree of protection in comparison with extensive armor. Since nowadays fights (especially fight against terrorism) often take place in town environment, a lot of attention is focused on the development of the near-zone protection. The ADS of this type detect the threat missiles and defuse them in very close vicinity (1-3 m) from the protected vehicle. The detection can be performed by a microwave multi-sensor system, [1] and [2].

Such sets of sensors can be described as a microwave "curtain" uncurled alongside the vehicle. Any missile flying through this "curtain" generates radar echoes, i.e. signals, which can be used for its detection. Fig. 1 shows example of radar output signal processed into a spectrogram of Doppler frequencies (Doppler signatures) corresponding to a flight of a long missile through the "curtain" right under one of microwave sensors.

If a simple flying target was detected, its spectrogram should appear as a section of an approximately horizontal line corresponding to the Doppler frequency shift. This shift is given in any textbook on radar as

$$\Delta\tilde{f} = 2f_0\frac{v_r}{c} \tag{1}$$

where v_r stands for radial velocity of the moving target and c is velocity of the light and f_0 stands for the transmitter frequency.

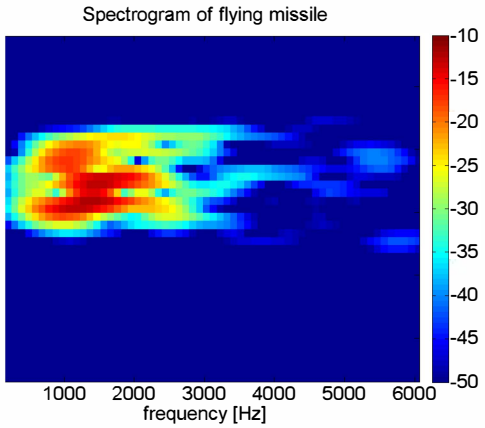

Fig. 1. Spectrogram of power density [dBW/Hz] received during a shot missile flying through a microwave curtain, trajectory incident with the vehicle, X-band radar.

As can be seen at Fig. 1, measured spectrograms do not correspond to such an assumption. Instead of a single (Doppler) line, a "cloud" of frequencies can be seen.

Origins of this cluster can be explained by the fact that the missile is a) much longer than the wavelength, and b) each part of the missile is "seen" by the radar under different angle β. Since any generated Doppler frequency shift is a function of radial velocity, proportional to cos (β) (shown at Fig. 2), a cluster of different output frequencies appears. The frequency "cloud" influences further signal processing to a substantial degree.

During development of an ADS, all potential elevations and azimuths of the missile approaching the microwave "curtain" must be taken into account. Missiles moving at non-incident trajectories, as well as ordinary bullets, should not trigger active countermeasures. Practical measurements at army shooting range are rather costly and time-consuming. Accurate computer modeling of radar output signals can reduce the number of required shots. Since the searched for signals depend on distribution of the EM fields in the vicinity of the objective fast-moving targets, a dynamic EM field modeling has to be used.

Doppler effect has been observed and described in the first half of 19-th century. The frequency shift caused by Doppler effect has been widely used to distinguish moving

978-88-907018-3-2/13 ©2013 IEEE

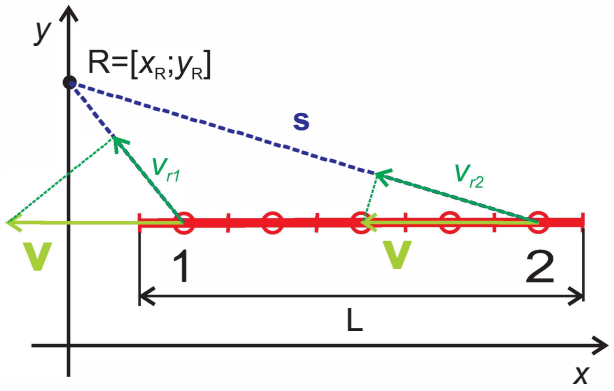

Fig. 2. Situation when the missile appears to be illuminated by a radar beam of variable frequency

targets from steady ones. Within the last two decades, more complex problems have been studied. The Doppler signatures received from bodies possessing moving parts ("Micro-Doppler Effect") were investigated. The results have been applied to distinguish echoes from walker hands [3], and to describe reflections from a (moving) helicopter rotor [4]. Numerous works have been focused on Doppler spectra within ultrasound bands, especially aiming at medical applications [5], [6]. Doppler spectrum of ideal point-target in the near field has been investigated [7]. No published results corresponding to radiation/scattering from fast moving and relatively long conductive objects in the vicinity of a radar sensor are known to the authors so far. The aim of this paper is to contribute to filling this gap.

II. Problem Description

The whole missile is of a very complex shape, which makes it complicated to deal with. As a first approximation, a thin conductive wire was used instead to examine the behavior of moving target Doppler signatures. The remaining problem is still complex enough. As shown in [8], the problem should be solved in the reference frame of the moving target.

Imagine a voyager traveling at the target approaching the bistatic radar. Within his reference frame, the target appears to be illuminated by a radar beam of variable frequency. Depending on the angle of incidence, the received frequency is the highest on the back of the target. The situation is depicted at Fig. 2.

Let us first consider illumination from the transmitting antenna T at the point denoted by "1" only. The incoming beam emited by transmitter induces current flow at the point of incidence and consequently at the whole wire surface. This current gives origin to radiation from the wire, within the reference frame of the voyager, there is (so far) one frequency only. However, in the reference frame of the receiving antenna R radial velocities of different locations at the wire are not equal, and therefore the received signal would contain a certain frequency band.

Let us repeat this consideration with a second beam, incident with the missile at point "2". The situation is similar, now we have two frequencies in the reference frame of the voyager. Again, the radiation is received at the receiver location as a frequency band. The two frequency bands are partially overlapping, causing constructive or destructive interference at certain frequencies. These frequencies depend at the location of the target.

In reality, the target is illuminated over its whole length, so that the observer would experience currents excited over a continuous range of frequencies. The signal received at receiver would become quite complex.

It should be mentioned that the voyager would also notice, that the target, once illuminated at any point at certain frequency, would radiate this frequency even after this illumination was terminated (the target has already left the location corresponding to that frequency, but the energy acquired has not been radiated nor converted into heat loss yet). In a case of very fast targets, this should be taken into account. Our calculations do neglect this effect as the damping is fast enough.

The incident wave feeds electric oscillations of the whole target, so that virtually any point on it is fed by a frequency spectrum arising from (monochromatic) radar irradiation. From the electromagnetic point of view, the moving string could be cut into a set of small (close to elementary) dipoles. The received signal is calculated as a sum of the electromagnetic waves radiated from each elementary dipole. This includes the phenomenon that the signal from each part of the flying wire is seen under a different angle β and from a different distance, which affects a Doppler frequency shift.

III. Electromagnetic Modeling

A. The Electric Field Integral Equation

The EFIE [9] can be formulated by employing a boundary condition for the tangential incident ($\mathbf{E}^i$) and a scattered ($\mathbf{E}^s$) electric field on the perfect electric conductor (PEC):

$$\mathbf{n}_0 \times \mathbf{E}^i(\mathbf{r}') = -\mathbf{n}_0 \times \mathbf{E}^s(\mathbf{r}') = \mathbf{n}_0 \times \mathcal{L}\big(\mathbf{J}(\mathbf{r}')\big). \quad (2)$$

where $\mathbf{r}' \in \Omega$, Ω is the selected structure to be analyzed. The integro-diferential operator $\mathcal{L}$ can be defined as

$$\mathcal{L}\big(\mathbf{J}\big) = \jmath\omega\mathbf{A}(\mathbf{J}) + \nabla\phi(\mathbf{J}), \quad (3)$$

where $\mathbf{A}(\mathbf{J})$ and $\phi(\mathbf{J})$ are vector and scalar potentials[1] respectively [9]. Formulation (3) is also known as the Mixed Potential Integral Equation (MPIE). Physically, $-\mathcal{L}\big(\mathbf{J}\big)$ gives the scattered electric field intensity and therefore the operator $\mathcal{L}$ has the characteristic of impedance

$$\mathbf{Z}(\mathbf{J}) = \mathbf{n}_0 \times \mathcal{L}\big(\mathbf{J}\big). \quad (4)$$

Once again we note here that we solve the whole problem in the reference frame of the target. Thus, the object Ω is stationary for calculation of (2). Impedance matrix of the wire can be easily obtained by Method of Moments (MoM, [10])

[1]Note here, that both vectors and matrices are marked in bold in this paper.

and than the inversion can be performed to obtain the currents flowing on the shape Ω

$$\mathbf{J}_s = \mathbf{Z}^{-1}\mathbf{E}^i, \tag{5}$$

where $\mathbf{J}_s$ is the surface current to be calculated. The column vector $\mathbf{E}^i$ represents the incident plane wave of different frequencies. This feeding scenario can be understood as a series of voltage gap generators [9], representing the Huyghens principle [11] of moving object[2].

B. The Method of Moments

From practical point of view, the implemented MoM is thin-wire approximation with so-called reduced kernel [13]. The basis functions are piecewise constant, the testing functions are realized by point-matching method [14] as Dirac impulses. The resulting matrix is symmetrical. The inversion (5) is executed via Gaussian elimination with partial pivoting [15] in Matlab [16].

The singular (self-) terms [14] were treated according [17]. This approach includes expansion the self-term in a MacLaurin series, singularity extraction and integrating of elliptic integral of the first kind.

Implemented thin-wire MoM was verified by an example of half-wave thin-wire dipole, including the convergence study of the input impedance. Presented method is also suitaible to make use of HPC (each frequency step is computed by different processor) or GPU (properly vectorization of impedance matrix calculation opens new posibilities in speed-up of the MoM for given frequency step).

Some further remarks dealing with discretization are mentioned at the end of the paper.

C. Doppler Spectrum

The Doppler effect is observed whenever the source of waves is moving with respect to an observer. It can be described as the effect produced by a moving source of waves in which there is an apparent upward shift in frequency for observers towards whom the source is approaching and an apparent downward shift in frequency for observers from whom the source is receding. It is important to note that the effect does not result because of an actual change in the frequency of the source.

Further, radar transmits an electromagnetic signal to the target and receives a returned signal from the target. If the target is moving, the frequency of the received signal will be shifted from the frequency of the transmitted signal. The Doppler frequency shift (1) is determined by the radial velocity (6) of the moving target

$$v_r = \frac{\mathbf{v}\cdot\mathbf{s}}{\|\mathbf{s}\|} \tag{6}$$

where $\mathbf{v}$ stands for velocity of the flying target and $\mathbf{s}$ stands for position vector (if reference point will be considered on the target), as can be seen at Fig. 3.

[2]This principle was generalized as Equivalence method [12].

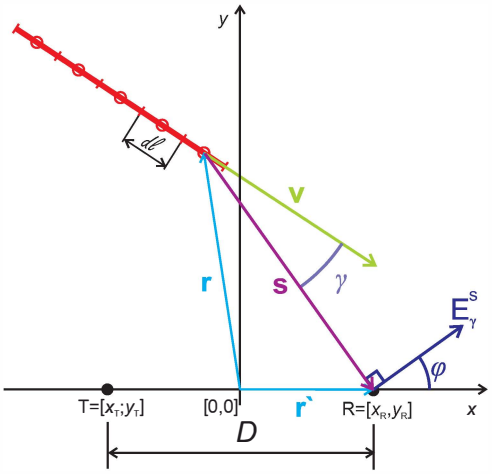

Fig. 3. Top view of a scene showing all the important parameters

The Doppler spectrum becomes apparent when the target is much longer than the wavelength. The radial velocity of the received signal from each distance on the target is different. This phenomenon causes the resulting signal in the Doppler spectrum.

D. Superposition of Scattered Field in Receiver

The receiving antenna is close enough to observe different Doppler shifts from various parts of the target, but far enough (in comparison to wavelength and element length, $kr >> 1$) to receive only far-field radiated components. Having calculated current distribution, it is possible to express received electromagnetic wave on the antenna. As mentioned before, the electric field intensity can be calculated using elementary electric dipoles. Then the electric field intensity is given by

$$E^s_\gamma = j\frac{Z_0 dl}{4\pi}\sum_{m=1}^{M} I(m)k(m)\sin(\gamma(m))\frac{e^{-jk(m)\|\mathbf{s}(m)\|}}{\|\mathbf{s}(m)\|} \tag{7}$$

where Z_0 stands for the characteristic impedance of free space, k represents the wave number, β stands for the angle between $\mathbf{s}$ and $\mathbf{v}$ and the vectors $\mathbf{r}$ and $\mathbf{r}'$ making an angle ψ, as can be seen at Fig. 3

IV. EXAMPLE

Although the real situation at the battlefield is always a 3D one, the problem can be simplified to 2D in order to improve computational efficiency. As stated above, another approximation, a thin conductive wire was used.

The sensors (transmitter and receiver) are considered to be pointwise. The directional characteristic of each sensor is included. The target is flying perpendicularly to axis of the antennas in the same plane and flying through the middle of them.

This problem can be separated to three parts (steps). In the first step, the transmitter irradiates the flying target, the wire in this case. Results of the first step are the vector of Doppler

frequency with the number of samples on its length and the far electric field with the same length.

In the second step, the current distribution will be found on the flying target by the MoM. The flying target will be fed on every sample by the far electric field with different frequency dependent on vector of Doppler frequency. It is important to take only direct-target component of the far electric field. The result of the second step is the matrix of current distribution.

In the third step, the flying wire irradiates the receiver from each sample. The far electric field will be computed from each sample on the wire with respect to received frequency (eg. corresponding to the reference frame of the receiver).

A. Geometrical Arrangement

The top-view of the scene is depicted in Fig. 3. The antennas (T - transmitter, R - receiver) are situated in the distance D in agreement with Fig. 3 and the approaching target is represented by a red abscissa with length l.

Target moving along the axis is inclined with y axis angle θ. If the target moves from the right to the left, the angle θ is negative and vice versa. It will be marked like θ^- and θ^+. Vectors $\mathbf{v}$ and $\mathbf{r}$ are inclined to angle β, which can be written by

$$\cos\gamma = \frac{\mathbf{v}\cdot\mathbf{s}}{\|\mathbf{v}\|\,\|\mathbf{s}\|}, \tag{8}$$

The angle φ, see Fig. 3, is used for convert of E^s_β to longitudinal component E^s .

B. Problem Solution

The thin-wire is discretized to M samples. Each sample is fed by $\mathbf{E}^i$ from transmitter T with different frequency $f(m) = f_0 + \tilde{f}(m)$ where Doppler frequency shift can be writen

$$\tilde{f}(m) = f_0\frac{v_r(m)}{c} \tag{9}$$

This results, M current distribution appear on length of the thin-wire. Every sample on every frequency of current distribution is a source for an incident wave in the reference frame of the receiver. The matrix $(m \times m)$ of Doppler frequency shifts appears here. Depending on time, one can obtain

$$\tilde{\mathbf{f}}(n,m,t) = \begin{bmatrix} \tilde{f}_{11}(t) & \tilde{f}_{12}(t) & \dots & \tilde{f}_{1m}(t) \\ \tilde{f}_{21}(t) & \tilde{f}_{22}(t) & \dots & \tilde{f}_{2m}(t) \\ \vdots & \vdots & \ddots & \vdots \\ \tilde{f}_{n1}(t) & \tilde{f}_{n2}(t) & \dots & \tilde{f}_{nm}(t) \end{bmatrix} \tag{10}$$

As well as the matrix of Doppler frequency shift was obtained, the matrix electric field intensity follows:

$$\mathbf{E^s}(n,m,t) = \begin{bmatrix} E^s_{11}(t) & E^s_{12}(t) & \dots & E^s_{1m}(t) \\ E^s_{21}(t) & E^s_{22}(t) & \dots & E^s_{2m}(t) \\ \vdots & \vdots & \ddots & \vdots \\ E^s_{n1}(t) & E^s_{n2}(t) & \dots & E^s_{nm}(t) \end{bmatrix} \tag{11}$$

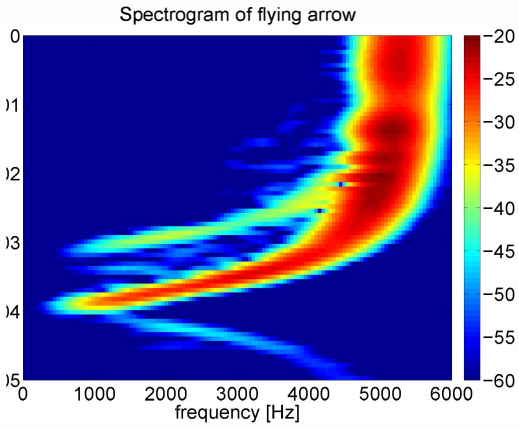

Fig. 4. Spectrogram of power density [dBW/Hz] taken during an arrow flying through radar sensors (measurement). At the time of 0.03 s the target head gets past the antenna plane. Due to finite antenna Front-to-Back Ratio, the resulting spectrogram is affected by sidelobes since then.

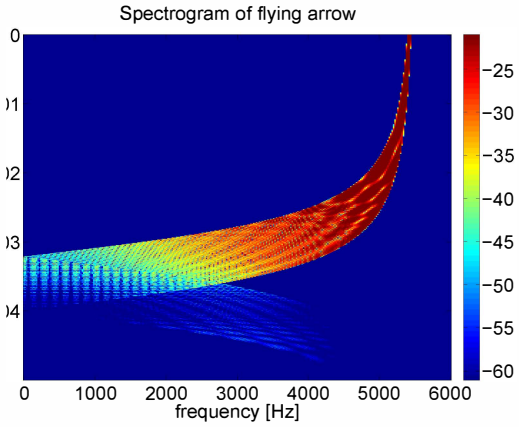

Fig. 5. Spectrogram of power density [dBW/Hz] taken during an arrow flying through radar sensors (simulation).

The matrix of Doppler frequency shifts is used as a mask to select elements from the matrix of electric field intensities. For elements of the frequency matrix, corresponding with interval $\langle f_\mathcal{D} - \Delta f; f_\mathcal{D} + \Delta f\rangle$, sum of elements of the electric field intensity matrix with same index is a result

$$E^s(f_\mathcal{D},t) = \sum_{i,j}\mathbf{E}^s(f_\mathcal{D} - \Delta f < \tilde{f}_{ij} < f_\mathcal{D} + \Delta f, t), \tag{12}$$

where Δf is selected half-range of sensitivity (in this case 10 Hz) and $f_\mathcal{D} \in \{10, 30, 50 \dots F\}$. The results of this computation can be seen at Fig. 5.

C. Measurement and Simulation

In order to compare simulations to measurements, a simple target Doppler signature was needed. Measured signal was obtained by firing a metallic arrow $L = 0.585$ m from a crossbow between the antennas in the distance $D = 1$ m with the velocity around $v = 80$ m/s. The diameter of the arrow is about $a = 5$ mm (circumference is small enough to

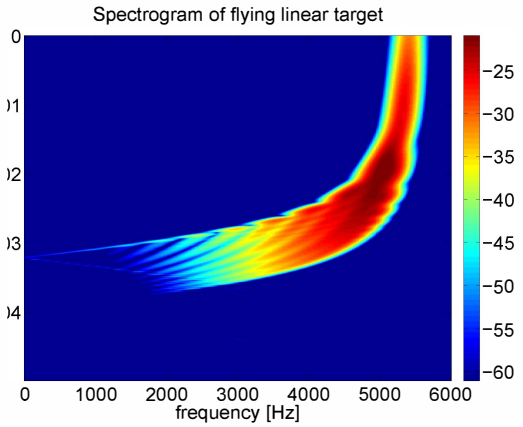

Fig. 6. Spectrogram of power density [dBW/Hz] taken during an arrow flying through radar sensors (simulation with convolution).

allow longitudinal oscillation modes only). The results of the measurement Fig. 4 should be comparable to the simulation.

As could be seen in Fig. 4, the Doppler frequency shift of target for far distance corresponds to flight velocity. Once the target approaches the sensors, the Doppler frequency shift decreases down to zero. An interesting effect, near the sensor, can be seen on the Doppler signature of signal in Fig. 4.

Simulated signal is obtained using the same input parameters as the measurement. The thin-wire of length $L = 0.585$ m and radius $a = 10$ μm with the velocity $v = 80$ m/s was discretized to $M = 200$ segments. The echo from target is discretized in time (by sampling frequency), the Doppler frequency and the amplitude of the electric fields intensity, which are depicted by the spectrogram, are interdependent. As simulation computes a contribution of each elementary dipole, the number of incoming waves is similar for all positions, so there is a problem with received Doppler frequency shift discretization. The frequency band has been divided into 20 Hz wide subintervals. Power contributions falling into the same interval have been added to obtain resulting spectrum level.

Both measured and simulated results have been processed using a Gauss window in order to provide for comparison. Fig. 6 shows simulation result, comparable with measured results plotted in Fig. 4.

V. Conclusion

Echoes resulting from a flight of a target close to a bistatic radar have been investigated in 2D. The problem has been simplified to long thin targets (wires). The Method of Moments used in the reference frame of the target proved to be an efficent tool for current distribution determination.

Simulation results compare well with measured ones and enable better understanding of the problem and improvement in ability to distinguish dangerous targets from ordinary ones.

More complex simulations in 3D, providing for complex shape targets using RWG functions [18] are underway.

VI. Acknowledgment

This work was supported by the Grant Agency of the Czech Technical University in Prague, grant No. SGS12/142/OHK3/2T/13.

References

[1] Hudec P., Raboch J., Randus M., Hoffmann K., Holub A., Svanda M., Polivka M., *Microwave Radar Sensors for Active Defense Systems*, Proceedings of the EuRAD conference, Rome 2009.

[2] Hudec P., Plasil J., Dohnal P., *Digital Signal Processing Applied to Radar Sensors Operated in Active Defense Systems*, Proceedings of the EuRAD conference, Paris 2010.

[3] Chen C. V., *The Micro-Doppler Effect in Radar*, Artech House, Boston 2011

[4] Green H. E., "Electromagnetic Backscattering from a Helicopter Rotor in the Decametric Wave Band Regime", *IEEE Trans. On Antennas and Propagation*, Vol. 42, No. 4, April 1994, pp. 501-509

[5] Censor, D.; Newhouse, V.L.; Vontz, T.; Ortega, H.V.: "Theory of ultrasound Doppler-spectra velocimetry for arbitrary beam and flow configurations". *IEEE Trans. on Biomedical Engineering*, Vol 35 (1988) , No. 9, pp.740-751.

[6] Denardo, S.J.; Talbot, L.; Hargrave, V.K.; Fitzgerald, P.J.; Selfridge, A.R.; Yock, P.G.:. "Analysis of pulsed wave Doppler ultrasound spectra obtained from a model intracoronary catheter". *IEEE Trans. on Biomedical Engineering*, Vol. 41 (1994), No. 7., pp. 635-648.

[7] PAN Xi, CUI Zhan-zhong, XU Li-xin, *Near Field Doppler Modeling and Simulation for Air Target*, 1-4244-2386-6/08/ 2008 IEEE.

[8] Roberto D. Graglia; Angelo Freni; Giuseppe Pelisi:. "A finite element approach to the electromagnetic Interaction with Rotating Penetrable cylinders af arbitraty cross section". *IEEE Trans. on antennas and propagation*, Vol. 41 (1993), No. 5., pp. 635-650.

[9] C. A. Balanis, *Advanced Engineering Electromagnetics*, Wiley, 1989.

[10] R. F. Harrington, *Field Computation by Moment Methods*, Wiley - IEEE Press, 1993.

[11] C. Huygens, *Traite de la Lumiere*, Leyeden, 1690.

[12] S. A. Schelkunoff, *Some Equivalence Theorems of Electromagnetics and Their Application to Radiation Problems*, Bell System Tech., Vol. 15, pp. 92-112, 1936.

[13] D. B. Davidson, *Computational Electromagnetics For RF and Microwave Engineering*, Cambridge Univ. Press, 2005.

[14] R. F. Harrington, "Matrix Methods For Field Problems", *Proc. of IEEE*, vol. 55, no. 2, pp. 136-149, Feb. 1967.

[15] A. F. Peterson, S. L. Ray, R. Mittra, *Computational Methods for Electromagnetics*, Wiley - IEEE Press, 1998.

[16] The Matlab. [Online]. Available: `http://www.mathworks.com/`

[17] Ch. M. Buttler, "Evaluation of Potential Integral at Singularity of Exact Kernel in Thin-Wire Calculations", *IEEE Trans. Antennas Propag.*, vol. 23, no. 2, pp. 293-295, March 1975.

[18] Rao, S. M., Wilton, D. R., Glisson, A. W.: "Electromagnetic Scattering by Surfaces of Arbitrary Shape", *IEEE Trans. AP*, Vol. 30, No. 3, pp. 409-418, May 1982.